Preprint Title	Hybrid Mode Atomic Force Microscopy of Phase-Modulation and Frequency-Modulation
Authors	Yasuhiro Sugawara, Tatsuya Yamamoto, Masato Miyazaki, Hikaru Nomura and Yan Jun Li
Publication Date	22 März 2022
Article Type	Full Research Paper
ORCID® iDs	Yasuhiro Sugawara - https://orcid.org/0000-0002-1233-5313

Hybrid Mode Atomic Force Microscopy of Phase-Modulation and Frequency-Modulation

Yasuhiro Sugawara [*1], Tatsuya Yamamoto[1], Masato Miyazaki[1], Hikaru Nomura[2], and Yan Jun Li[1]

1) Department of Applied Physics, Graduate School of Engineering, Osaka University, 2-1 Yamada-oka, Suita, Osaka 565-0871, Japan
2) Department of Materials Engineering Science, Graduate School of Engineering Science, Osaka University, 1-3 Yachinake-yama, Toyonaka, Osaka 560-0043, Japan

* Corresponding author

Electronic mail: sugawara@ap.eng.osaka-u.ac.jp

Abstract

We propose hybrid mode atomic force microscopy (AFM) of phase-modulation (PM) and frequency-modulation (FM) in constant amplitude (CA) mode to increase imaging speed of AFM in high-Q environments. We derive the relation among the phase shift, frequency shift and the tip-sample interaction force from the equation of motion for the cantilever in high-Q environments. The tip-sample conservative force is approximately given by the sum of the conservative force with respect to phase shift in PM mode and that with respect to frequency shift in FM mode. We preliminarily demonstrate that the hybrid AFM of PM and FM is a new very promising AFM operation mode that can increase imaging speed.

KEYWORDS:

atomic force microscopy (AFM), phase-modulation (PM), frequency modulation (FM), hybrid mode

Introduction

Various dynamic processes occur on the surface, such as surface diffusion, phase transitions, self-organization phenomena, chemical reactions, and etching [1]. These dynamical processes are of great fundamental and technological interest. The ability to study these process with high spatial and high temporal resolution is expected to provide access to non-equilibrium dynamins at the atomic level. Atomic force microscopy (AFM) not only can image atoms and molecules on the surface with ultimate spatial resolution [2-5], but also manipulate [6, 7] and characterize substances [8, 9]. Thus, AFM is now an indispensable nanoscale tool in surface science. However, the time resolution of AFMs operating in vacuum is one of their most severe limitations, since the typical image acquisition times are of the order of 10 seconds or longer. High-speed AFM operating in low-Q environment has been developed [10, 11], but high-speed AFM operating in high-Q environment has not been developed. Therefore, developing an AFM capable of high-speed imaging in high-Q environment is one of the most important technical challenges.

As the operating mode of AFMs, three operating modes such as amplitude modulation (AM) [10, 12, 13], frequency modulation (FM) [14, 15] and phase modulation (PM) [16-21] modes haven been used. In AM-AFM, a cantilever is always driven at/near the resonance frequency (f_0) with an external oscillator. The tip-sample interaction is

measured by the change (ΔA) in the oscillating amplitude. In AM-AFM, in which the cantilever is externally driven in constant excitation amplitude (CE) mode, the nonlinearity of the tip-sample interaction force leads complicated dynamical behaviors such as hysteresis and bistability [22], because two stable oscillation states coexist depending on the driving force and tip-sample distance [23]. In addition, In AM-AFM, the time constant τ_{AM} of the transient response of ΔA to the force changes is given by $\tau_{AM} = 2Q/f_0$, which becomes longer with increasing Q-factor [10]. This prohibits the use of AM-AFM in vacuum and limits the imaging speed in air.

In FM-AFM, a cantilever is always driven at the resonance frequency on the basis of a self-driven oscillator. The tip-sample interaction is measured by the frequency shift (Δf) of the oscillating cantilever. In FM-AFM, the vibration amplitude of the cantilever is mostly kept constant using an automatic gain control (AGC) circuit. This constant amplitude (CA) mode can not only prevent the complicated dynamical behaviors such as hysteresis and bi-stability, but also measure the conservative and dissipative interaction forces independently. In FM-AFM, the time constant τ_{FM} of the transient response of Δf to the force changes is given by $\tau_{FM} = 1/f_0$, which is not influenced by the Q-factor of the cantilever. Thus, FM-AFM can operate in high Q environments such as in a vacuum, resulting in extremely high force sensitivity and spatial resolution. However, τ_{FM} is often

practically longer than this prediction ($1/f_0$) due to the delay caused by the self-excitation circuit (that is, the phase feedback loop). This delay is especially noticeable when a phase-locked loop (PLL) circuit with bandwidth typically less than 1 kHz is involved in the self-excitation circuit [15]. Hence, the imaging speed is much slower than that expected from τ_{FM}.

In PM-AFM, a cantilever is driven at the fixed resonance frequency with an external oscillator. The tip-sample interaction is measured by the phase shift ($\Delta\phi$) of the oscillating cantilever. In PM-AFM operating in a constant excitation (CE) mode, complex dynamic behaviors, such as hysteresis and bistability, remain a problem [23]. In PM-AFM operating in the constant amplitude (CA) mode, in contrast, such the instabilities in nonlinear cantilever dynamics can be eliminated and the quantitative spectroscopy curve can be obtained for the tip–sample distance [18]. In addition in PM-AFM, the time constant τ_{PM} of the transient response of $\Delta\phi$ to the force changes is given by $\tau_{PM} = 1/f_0$, which is not influenced by the Q factor of the cantilever. These features suggest that the application of PM-AFM in CA mode is advantageous in order to realize high speed imaging in high-Q environments such as in a vacuum as well as in low-Q environments such as in a liquid. So far, the performance of PM-AFM in CA mode in low-Q environments has been investigated [16-22], but the performance of PM-AFM in CA

mode in high-Q environments has hardly been studied.

In this paper, to increase the imaging speed of AFMs operating in high-Q environments, we propose a hybrid AFM that utilizes the advantages of PM-AFM, i.e., fast transient response, and FM-AFM, i.e., the cantilever is always excited near its resonant frequency. First, we discuss the limitations of PM-AFM operation in high-Q environments. Then, we propose to utilize hybrid technique of PM and FM mode operation in high-Q environments to exceed the limitation. We derive the relation among the phase shift, frequency shift and the tip-sample interaction force from the equation of motion for the cantilever. We show that the tip-sample conservative force is approximately given by the sum of the conservative force with respect to phase shift in PM mode and that with respect to frequency shift in FM mode. We preliminarily demonstrate that the hybrid mode AFM of PM and FM is a new very promising AFM operation mode that can increase imaging speed.

Hybrid mode of PM and FM that exceeds the limitations of PM mode in high Q-environments

We discuss the limitations of PM mode in high-Q environments and propose the hybrid mode of PM and FM hybrid mode that exceed these limitations. Figure 1 shows

the phases (ϕ) of the oscillating cantilever as a function of the driving frequency (f). The resonance frequency at which the phase ϕ is $-\pi/2$ is shifted by the tip-sample interaction. f_0 is the resonance frequency of the cantilever when there is no tip-sample interaction (black line), while f_1 and f_2 are the resonance frequencies of the cantilever when there is tip-sample interaction (red and blue lines, respectively). In PM-AFM, the driving frequency is set to the fixed frequency at/near the resonance frequency f_0 at which the phase is $\phi=-\pi/2$. When tip-sample force interaction becomes strong, the frequency at which the phase is $\phi=-\pi/2$ changes to $f_1=f_0+\Delta f_{01}$, where Δf_{01} is the frequency shift of the cantilever. The tip-sample interaction is measured by the phase shift ($\Delta\phi_{01}$) of the oscillating cantilever at f_0.

The minimum detectable force of PM-AFM in high-Q environments is given by

$$\delta F_{PM} = \sqrt{\frac{k k_B T}{Q^2}}, \qquad (1)$$

where k and Q are the spring constant and the natural quality factor (Q-factor) of the cantilever, respectively. k_B and T are the Boltzmann constant and the absolute temperature, respectively. Here, noise arising from the cantilever deflection sensor is assumed to be much lower than that from the thermal Brownian motion of the cantilever. This equation means the advantage that high force sensitivity can be obtained by increasing Q-factor. However, increasing Q-factor has the disadvantage of limiting the available frequency

shift Δf_{01}, which is induced by the tip-sample interaction, and the following condition must be satisfied for available frequency shift Δf_{01}, because the slop of the phase ϕ with respect to the frequency f at f_0 depends on the Q-factor Q,

$$|\Delta f_{01}| < \frac{f_0}{2Q}. \qquad (2)$$

This condition is easily satisfied in low-Q environments such as in solutions, but difficult to satisfy in high-Q environments such as in a vacuum. For example, under the typical imaging conditions in vacuum, for a typical cantilever with Q=20,000 and f_0=300 kHz in vacuum, the maximum available frequency shift $|\Delta f_{01}|$ is only 7.5 Hz, which is unusable for the most high resolution imaging.

One possible way to satisfy the condition of PM mode in Eq. (2) in high-Q environments is to use hybrid technique of PM and FM modes. That is, as shown in Fig. 1, first, the limitation of the available frequency shift is resolved by changing the driving frequency f_0 to f_1 by FM mode under weak feedback conditions. Second, by measuring the phase shift ($\Delta\phi_{12}$) at f_1 by PM mode, the interaction between the tip and sample can be determined by the frequency shift (Δf_{01}= f_1-f_0) and phase shift ($\Delta\phi_{12}$). Hence, the distance between the tip and the sample is controlled by the sum of the feedback signal for the phase shift ($\Delta\phi_{12}$) and the feedback signal for the frequency shift (Δf_{01}). This hybrid mode of PM and FM has the advantage of increasing the imaging speed because it does

not need to wait for the transient response of the frequency shift in PLL as in the FM mode.

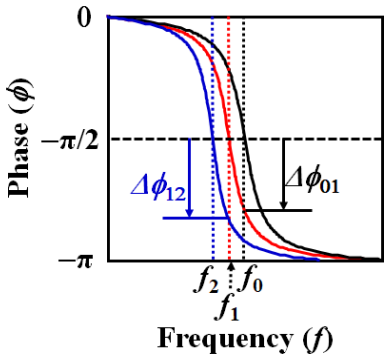

Figure 1: Phase of the oscillating cantilever as a function of the driving frequency. In hybrid mode of PM and FM, by changing the driving frequency f_0 to f_1 using the FM mode under the weak feedback condition, the limitation of the available frequency shift can be solved, and by measuring the phase shift ($\Delta\phi_{12}$) at f_1 using the PM mode, the tip-sample interaction can be determined from the frequency shift (f_1-f_0) and the phase shift ($\Delta\phi_{12}$).

Hybrid AFM system of PM and FM

Here, we consider the configuration to realize a hybrid mode of PM and FM. Figure 2 shows a block diagram of the proposed hybrid-mode AFM of PM and FM. Its configuration is very similar to FM-AFM that uses a PLL circuit in the self-excitation

loop. The cantilever is driven with a voltage controlled oscillator (VCO) at a resonance frequency f. The cantilever deflection is detected with a deflection sensor such as an optical beam deflection sensor. The amplitude A and phase ϕ of the oscillating cantilever are measured with a lock-in amplifier. The phase signal is fed into a proportional-integral-differential (PID) controller to control the input voltage of VCO, and the frequency shift Δf of the cantilever is measured. The oscillation amplitude A is maintained at constant value with AGC circuit using a multiplier and a PID controller in CA mode. The frequency shift Δf and the phase shift $\Delta\phi$ are separately connected to feedback circuits, and AFM images are obtained from the sum of these two feedback outputs. If the feedback on $\Delta\phi$ or Δf does not act, the system becomes FM- or PM-AFM, respectively.

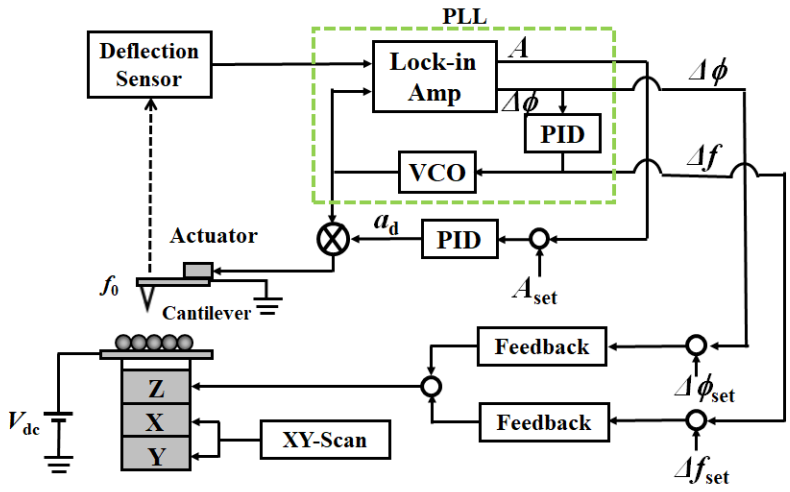

Figure 2: Block diagram of the hybrid mode AFM of PM and FM.

Theory of phase shift and frequency shift of hybrid mode AFM of PM and FM

Here we theoretically consider the relationship between tip-sample interaction force and the phase and frequency shifts of the cantilever, and show the operation by the hybrid mode of PM and FM is possible. The motion of the oscillating cantilever can be expressed by the following equation:

$$m\ddot{z}(t) + \frac{2\pi f_0 m}{Q}\dot{z}(t) + kz(t) = F\cos(2\pi f t) + F_{ts}. \qquad (3)$$

Here, m, f_0, and f are the effective mass, the resonance frequency and the driving frequency of the cantilever, respectively. F and F_{ts} are the driving force of the cantilever and the tip-sample interaction force, respectively. The cantilever deflection signal $z(t)$ in the steady state is given by

$$z(t) = A_0\cos(2\pi f t + \phi), \qquad (4)$$

where A_0 and ϕ are the amplitude of the oscillating cantilever and the phase difference between the driving and the deflection signals, respectively. Inserting Eq. (4) into Eq. (3), multiplying both side of the resulting equation by $\cos(2\pi ft+\phi)$ and $\sin(2\pi ft+\phi)$, and then integrating over an oscillation period, one can obtain two general analytical relations for the phase shift as follows:

$$F\cos\phi = kA_0\left\{1 - \left(\frac{f}{f_0}\right)^2\right\} - F_c, \quad (5)$$

$$F\sin\phi = kA_0\frac{1}{Q}\left(\frac{f}{f_0}\right) - F_d, \qquad (6)$$

where F_c and F_d are the f component of the Fourier series for the conservative and dissipative tip-sample interaction forces, respectively, expressed as follows:

$$F_c = 2f\int_0^{1/f} F_{ts}\cos(2\pi ft+\phi)dt, \qquad (7)$$

$$F_d = 2f\int_0^{1/f} F_{ts}\sin(2\pi ft+\phi)dt. \qquad (8)$$

The phase shift $\Delta\phi$ of the cantilever is defined as phase shift from -π/2 phase delay of the cantilever oscillator signal as follows:

$$\Delta\phi = \phi - (-\pi/2) \qquad (9)$$

On the basis of Eqs. (5), (6) and (9), $\Delta\phi$ is given by

$$\Delta\phi \approx \tan(\Delta\phi) = \frac{kA_0\{1-(f/f_0)^2\}-F_c}{kA_0(1/Q)(f/f_0)+F_d} \qquad (10)$$

This equation indicates that the phase shift $\Delta\phi$ depends on both conservative force F_c and dissipative force F_d. From Eq. (10) and $f = f_0+\Delta f$, the conservative force F_c is expressed as follows:

$$F_c \approx -\left\{kA_0\frac{1}{Q}\left(1+\frac{\Delta f}{f_0}\right)+F_d\right\}\Delta\phi - 2kA_0\frac{\Delta f}{f_0} \qquad (11)$$

In the PM mode, the cantilever is driven at a fixed resonant frequency f_0 (Δf =0). In this case, the second term in Eq. (11) is zero, and assuming that the dissipative force is very small ($F_d\approx 0$), the conservative force F_{cPM} is given only by the phase shift $\Delta\phi$ as follows:

$$F_{cPM} \approx -kA_0\frac{\Delta\phi}{Q} \qquad (12)$$

In FM mode, on the other hand, the cantilever is always driven at the resonance frequency (ϕ =–π/2, $\Delta\phi$ =0). In this case, the first term in Eq. (11) is zero and the conservative force F_{cFM} is given only by the frequency shift Δf as follows:

$$F_{cFM} \approx -2kA_0\frac{\Delta f}{f_0} \quad (13)$$

By comparing Eq. (11) with Eqs. (12) and (13), the following relationship can be obtained.

$$F_c \approx -kA_0\frac{\Delta\phi}{Q} - 2kA_0\frac{\Delta f}{f_0} \approx F_{c_{PM}} + F_{c_{FM}}, \quad (14)$$

where the approximation $\Delta f/f_0 << 1$ is used. Equation (14) shows that the conservative force F_{c} is given by the two physical quantities of the oscillating cantilever: the phase shift $\Delta\phi$ and the frequency shift Δf. In other words, this equation means that it is possible to operate in the hybrid mode, which is a combination of PM and FM modes.

It should be noted that in the hybrid mode of PM and FM, the set value of the phase shift feedback can be set to zero. The time constant τ_{PM} of the transient response of $\Delta\phi$ to the force changes in PM mode is much shorter than the time constant τ_{FM} of the transient response of Δf to the force changes in FM mode. Therefore, in FM mode, the feedback response of the tip-to-sample distance is slower, but in the hybrid mode of PM and FM with zero phase shift setpoint, the feedback response of the tip-to-sample distance is faster because the feedback response on the phase shift is added. Furthermore, the minimum detectable force is proportional to $B^{0.5}$ in PM mode [16, 17], while it is proportional to

$B^{1.5}$ in FM mode [24], where B is the bandwidth of the deflection sensor. These results suggest that the hybrid mode of PM and FM is a new very promising AFM operating mode that can significantly improve the PLL delay, which is a drawback of the FM mode, and increase the imaging speed of AFMs operating in high-Q environments.

Results and Discussion

By adding the feedback output from the PM mode to the feedback output from the FM mode, we experimentally investigated whether the hybrid mode of PM and FM can operate stably, and investigated the effectiveness of the hybrid mode of PM and FM with respect to the FM mode. Figure 4(a) shows AFM image of Si(111)-surface measured with FM mode. The AFM image was obtained from the feedback output of the frequency shift in the attractive force region under weak feedback conditions where the tip-sample distance control was not so sufficient. In Fig. 4(a), atomically flat terraces and steps on the Si surface are observed, but not clearly. Step in particular are observed blurred. In contrast, Fig. 4(b) shows AFM image of Si(111)-surface measured with hybrid mode of PM and FM. The AFM image was obtained from the sum of two feedback outputs, one for the same weak feedback condition for the frequency shift and the other for the strong feedback condition for the phase shift. In Fig. 4(b), terraces and steps on the Si surface

was clearly observed. In particular, adsorbates (bright spots) on the terraces and steps are very clearly observed. As shown in the cross-sections in Figs. 4(c) and 4(d), the hybrid mode of PM and FM sharply images the atomic-scale steps and their vicinity on the Si surface compared to the FM mode. Thus, we succeeded in experimentally verifying that the hybrid mode of PM and FM works stably and that atomic-level features on the sample

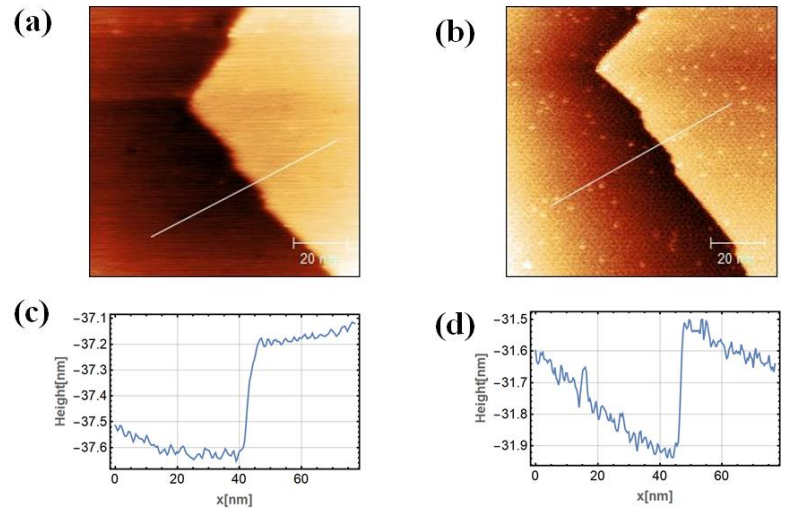

Figure 4: AFM topographic images of Si(111) surface measured by (a) FM mode and (b) hybrid mode of PM and FM, respectively. Cross-sectional profiles along the white lines in (a) and (b) measured by (c) FM mode and (d) hybrid mode of PM and FM, respectively. Spring constant, resonance frequency, Q-factor and vibration amplitude of the cantilever were k=26 N/m, f_0=242 kHz, Q=3600, and A = 10 nm, respectively. Frequency shift of the cantilever was Δf = -2.3 Hz in (a) and (b), and the phase shift was $\Delta\phi$ =0 Hz in (b).

surface can be observed with higher resolution than in the FM mode.

To increase the imaging speed of hybrid-mode AFM of PM and FM operating in a high Q environment, it is necessary to increase the speed of the various elemental technologies that make up the AFM. For example, higher frequency cantilevers, higher bandwidth displacement sensors, faster frequency, amplitude, and phase detection of cantilevers, wider bandwidth feedback circuits, and faster scanners. In particular, AFMs operating in a vacuum environment require the use of large, heavy specimen holders that enable heating and sputtering treatment of the specimen, making it difficult to increase scanner speed. In the future, the imaging speed of AFMs operating in a high Q environment could be further improved by replacing the scanner with a more rigid scanner with a higher resonant frequency.

Conclusion

We proposed to utilize hybrid technique of PM and FM modes to increase the imaging speed of AFM operating in high-Q environments. We theoretically investigated the performance of the hybrid mode AFM of PM and FM. We found the relation among the phase shift, frequency shift and the tip-sample interaction force from the equation of motion for the cantilever in high-Q environments. We found that the tip-sample

conservative force is approximately given by the sum of the conservative force with respect to phase shift in PM mode and that with respect to frequency shift in FM mode. Preliminary experiments have demonstrated that adding the feedback output of the phase shift from the PM mode to the feedback output of the frequency shift from the FM mode enables clearer imaging of atomic-scale features on the Si surface.

Replacing the sample scanner with a more rigid scanner with a higher resonance frequency could further improve imaging speed, even for AFMs operating in a high Q environment. Hybrid mode AFM with PM and FM could also further improve imaging speed for FM mode AFMs operating in low Q environments, such as in gaseous or liquid environments.

Experimental

Experiments were performed using custom-built AFM operating under ultrahigh vacuum (UHV) condition and at room temperature. Deflection of the cantilevers was measured using the optical beam deflection method. Frequency shift and phase shift of the oscillating cantilevers were measured by keeping the vibration amplitude constant with the oscillation controller (OC4 oscillation controller, SPECS). Hybrid AFM images of PM and FM were obtained from the sum of output signals of the two feedbacks (the

feedback controller and the generic PI controller, SPECS).

As a sample surface, a Si(111)-7×7 surface was used. The surface was prepared by thermal treatment of B-doped Si(111) sample. As a force sensor, we used a Si cantilever with spring constant of k=26 N/m, resonance frequency f_0=242 kHz. and Q factor of Q=3600. A vibration amplitude of the cantilever was A = 10 nm. Bias voltage between the tip and the surface was applied to compensate the contact potential difference between the tip and the surface.

Acknowledgments

The authors thank T. Yamanaka and Z. Zhang for conducting the AFM experiments.

Funding

This work was supported by JSPS KAKENHI Grant Numbers JP20K21128, JP21H04662.

References

1. Zangwill A. Physics at surfaces; Cambridge University Press, U. K., 1988.
2. Giessibl F. J. *Science* **1995**, 267, 68-71.
3. Sugawara Y.; Ohta M.; Ueyama H.; Morita S. *Science* **1995**, 270, 1646-1648.
4. Barth C.; Reichling M. *Nature*, **2002**, 414, 54-57.
5. Gross, L.; Mohn, F.; Moll, N.; Liljeroth, P.; Meyer, G. *Science*, **2009**, 325, 1110-1114. doi: 10.1126/science.1176210
6. Kawai, S.; Foster, A. S.; Canova, F. F.; Onodera, H.; Kitamura S.; Meyer, E. *Nature Commun.* **2014**, 5, 4403. doi: 10.1038/ncomms5403
7. J. Bamidele, J.; Lee, S. H.; Kinoshita, Y.; Turanský, R.; Naitoh, Y.; Li, Y. J.; Sugawara, Y.; Štich, I.; Kantorovich, L. *Nature Commun.* **2014**, 5, 4476. doi:10.1038/ncomms5476
8. Naitoh, Y.; Turanský, R.; Brndiar, J.; Li, Y. J.; Štich, I.; Sugawara, Y. *Nature Physics*, **2017**, 13, 663-667. doi: 10.1038/NPHYS4083
9. Adachi Y.; Wen H. F.; Zhang Q. Z.; Miyazaki M.; Sugawara Y.; Sang H.; Kantorovich L.; Štich I.; Li Y. J. *ACS Nano*, **2019**, 13, 6917-6924.
10. Ando, T. *Nanotechnology*, **2012**, 23, 062001. doi:10.1088/0957-4484/23/6/062001
11. K. Miyata, J. Tracey, K. Miyazawa, V. Haapasilta, P. Spijker, Y. Kawagoe, A. S.

Foster, K. Tsukamoto, T. Fukum, *Nano Lett.* **2017**, 17, 4083–4089. doi: 10.1021/acs.nanolett.7b00757

12. Kawai S.; Kawakatsu H. *Appl. Phys. Lett.*, **2006**, 89, 013108
13. Dagdeviren O. E.; Götzen J.; Hölscher H.; Altman E. I.; Schwarz U. D. *Nanotechnology* **2016**, 27, 065703. doi.org/10.1088/0957-4484/27/6/065703
14. Albrecht, T. R.; Grütter, P.; Horne, D.; Ruger, D. *J. Appl. Phys.* **1991**, 69, 668-673. doi: 10.1063/1.347347
15. Dürig U.; Steinauer H. R.; Blanc N. *J. Appl. Phys.* **1997**, 81, 3641-3651.
16. Kobayashi, N.; Li, Y. J.; Naitoh, Y.; Kageshima, M.; Sugawara, Y. *Jpn. J. Appl. Phys.* **2006**, 45, L793-L795. doi: 10.1143/JJAP.45.L793
17. Fukuma, T.; Kilpatrick, J. I.; Jarvis, S. P.; *Rev. Sci. Instrum.* **2006**, 77, 123703. doi: 10.1063/1.2405361
18. Sugawara, Y.; Kobayashi, N.; Kawakami, M.; Li, Y. J.; Naitoh,Y.; Kageshima, M. *Appl. Phys. Lett.* **2007**, 90, 194104. doi: 10.1063/1.2737907
19. Li, Y. J.; Kobayashi, N.; Nomura, H.; Naitoh, Y.; Kageshima, M.; Sugawara, Y. *Jpn. J. Appl. Phys.* **2008**, 47 6121-6124. doi: 10.1143/JJAP.47.6121
20. Hölscher, H. *J. Appl. Phys.* **2008**, 103, 064317. doi: 10.1063/1.2896450
21. Van, L. P.; Kyrylyuk, V.; Thoyer, F.; J. Cousty, J. *J. Appl. Phys.* **2008**, 104, 074303.

doi: 10.1063/1.2986152

22. Aimé, J. P.; Boisgard, R.; Nony, L.; Couturier, G. *Phys. Rev. Lett.* **1999**, 82, 3388. doi: 10.1103/PhysRevLett.82.3388

23. García R.; Paulo, A. S. *Phys. Rev. B.* **1999**, 60, 4961. doi: 10.1103/PhysRevB.60.4961

24. Kobayashi K.; Ya mada H.; Matsushige K. *Rev. Sci. Instrum.* **2009**, 80, 043708.